PAPER C

ENHANCED OIL RECOVERY MONITORING: AN APPLICATION OF ATTENUATION TOMOGRAPHY

Jerry M. Harris, Feng Yin* and Youli Quan

ABSTRACT

Crosswell attenuation tomography is used to image reservoir zones that were flooded by carbon dioxide. The swept zones contain mixtures of oil, water and carbon dioxide. Monitoring the saturation of these fluids is an important part of an enhanced oil recovery process. We estimate the changes in *P*-wave attenuation caused by the CO_2 injection process. Laboratory data on flooded cores are analyzed in support of the field data interpretation. We use a broad band amplitude spectrum method and the centroid frequency shift method to estimate the attenuation. These methods are applied to seismic waveforms recorded before and after the CO_2 injection.

We use synthetic simulation to verify the methodology, then apply the methods to real data from a CO_2 field pilot project. The synthetic and real data results indicate that it is possible to apply attenuation tomography methods to monitoring enhanced oil recovery processes for the purpose of detecting and imaging changes in reservoir storage and flow properties during the course of production. The results presented in this report illustrate the potential usefulness of crosswell and/or surface seismic techniques for routine monitoring applications.

* Now with Diasonics, 2860 De La Cruz Blvd, Santa Clara, CA 95050

INTRODUCTION

The processes by which oil is extracted from a reservoir are commonly divided into primary, secondary, and tertiary recovery. Following primary and secondary recovery, slightly more than half of the original oil often remains. The remaining oil is the target of tertiary recovery, also called enhanced oil recovery (EOR). Enhanced oil recovery processes are usually divided into three categories - miscible, chemical, and thermal processes (Broome et al., 1986). Most EOR processes share the feature that there is a narrow zone or front across which a crucial variable, either concentration or temperature, varies rapidly. A problem with all EOR processes is that the responsible engineers usually do not know where this front (of CO_2, chemical flooding or steam) is located between wells. If this information can be accurately determined, engineers can optimize strategies for placement of new wells, injection and production flow rates, and rate of injectants. An accurate analysis and monitoring of a reservoir would require understanding of its geology, the resident fluids and their behavior under the influence of injection and production activities. In this CO_2 pilot experiment, we are concerned with imaging the steady state changes in saturation following several cycles of a water-alternating-gas (WAG) injection process.

By recording two seismic profiles before and after an injection experiment, crosswell profiling can provide images of the flooded zone because the acoustic properties (e.g., velocity, attenuation, and reflectivity) change dramatically with injection. Significant changes in seismic attenuation associated with CO_2 injection are verified in this study. These changes are easily observed in time lapse imaging experiments. In this report, we concentrate on imaging the changes in attenuation due to CO_2. Attenuation is a very important parameter for the characterization of rock and fluid properties, e.g., saturation, porosity, permeability and viscosity. Attenuation appears to be more sensitive than velocity to some of these properties (e.g., Best et al., 1994).

Over the past decade, many methods have been developed, on the basis of seismic waveform or sonic logs, for estimating attenuation, and some preliminary experimental results have been published. These methods can be broadly divided into the time domain and frequency domain approaches. [Cheng et al, 1982, Engelhard et al, 1984]. At the present time, no method gives accurate estimates of absolute rock attenuation when the heterogeneity of the rock must be taken into account. There are many factors that contribute to this difficulty. For example, scattering, geometrical spreading, source and

receiver coupling, radiation patterns, transmission/reflection effects, and unknown source functions, etc.. Nevertheless, many of these difficulties can be minimized if not eliminated when utilizing two recordings, one before and one after the injection has taken place. Therefore, if we attempt to estimate the change in attenuation (i.e., relative attenuation) under time varying reservoir conditions, many factors that normally affect the estimation of absolute attenuation can be nearly eliminated. Relative attenuation can be estimated reliably in enhanced oil recovery monitoring.

In this paper, we investigate attenuation tomography to estimate the variation of the attenuation coefficient of 2-D inhomogeneous rocks in a reservoir experiencing carbon dioxide flooding. By using two broad band seismic data sets, one before and one after the CO_2 injection, we may use spectrum ratio and centroid frequency shift methods to estimate the integrated attenuation variation. Then we use tomographic reconstruction techniques to convert the integrated attenuation data to local attenuation variation in the reservoir area. We can set up a large linear system of equations for obtaining the 2-D attenuation distribution. Because the data usually contain coherent noise, we apply the Maximum Entropy Cambridge algorithm (Skilling, and Bryan, 1984) to solve the ill-posed system. From the time lapse attenuation tomography, we approach the goal of monitoring enhanced oil recovery.

We present the results of a simulation study, and preliminary results from a field study involving before and after CO_2 injection experiments. The results reveal a strong variation of *P*-wave attenuation caused by CO_2 injection.

MONITORING EOR WITH ATTENUATION TOMOGRAPHY

For the purpose of estimating attenuation, we assume that the process of wave propagation is described by linear system theory. If the amplitude of an incident wave is $S(f)$ and the medium/instrument response is $G(f)H(f)$, then the received amplitude spectrum $R(f)$ may be, in general, expressed as

$$R(f) = G(f)H(f)S(f) \tag{1}$$

where the factor $G(f)$ includes geometrical spreading, instrument response, source/receiver coupling, radiation patterns, reflection/transmission coefficients and the phase accumulation due to propagation, and $H(f)$ describes the attenuation effect on the

amplitude. Experiments indicate the attenuation is usually proportional to frequency, that is, we may write,

$$H(f) = \exp(-f\int_{ray} \alpha_0 dl) \tag{2}$$

where the integral is taken over the ray path and α_o is the attenuation coefficient defined by

$$\alpha_o = \frac{\pi}{Qv} \tag{3}$$

i.e., attenuation is linear proportional to frequency, where Q is the medium's quality factor and v is wave velocity. Note that our attenuation factor α_o is different from the usually defined attenuation coefficient $\alpha = \alpha_o f$. This linear frequency model is useful in demonstrating the spectral ratio and frequency shift methods. More complex models, for example, with higher power dependence on frequency, can be also considered in a similar way (Narayana and Ophir, 1983).

Our goal is to estimate the medium response $H(f)$ or more specifically the attenuation coefficient α_o, from knowledge of the input of the spectrum $S(f)$ and output spectrum $R(f)$. A direct approach is to solve equation (1) by taking the logarithm and obtain

$$\ln[\frac{GS(f)}{R(f)}] = (\int_{ray} \alpha_o dl) \cdot f. \tag{4}$$

Equation (4) may be used to estimate the integrated attenuation at each frequency and is called an amplitude ratio method. However, as described previously, the factor G lumps together many complicated processes, and is very difficult to determine. $S(f)$ is also unknown. This makes it very difficult to estimate the absolute attenuation. However, in the crosswell monitoring experiment, we have two seismic data sets. One data set is measured before CO_2 injection, the other after CO_2 injection. If we want to invert for relative attenuation, these factors can be eliminated. Next we will use the amplitude spectral ratio and centroid frequency shift methods to invert for the relative attenuation parameter.

SPECTRAL RATIO METHOD

From the before and after data sets, we can obtain the two spectra. We denote $R_1(f)$ and $R_2(f)$ to be the spectra of before and after CO_2 injection, respectively. So we have

$$\{\ln[GS_1(f)] - \ln[R_1(f)]\} = (\int_{ray} \alpha_{1o} dl) \cdot f \tag{5}$$

$$\{\ln[GS_2(f)] - \ln[R_2(f)]\} = (\int_{ray} \alpha_{2o} dl) \cdot f \tag{6}$$

where $S_2(f) = C \cdot S_1(f)$, and C is a constant used to account for a scale difference between the two experiments. From the above equation, we obtain,

$$Y(f) = a \cdot f - b \tag{7}$$

where, $Y(f) = \ln[R_1(f) / R_2(f)]$, $a = (\int_{ray} \Delta\alpha_o dl)$, and $\Delta\alpha_o = \alpha_{2o} - \alpha_{1o}$, which is the variation of the attenuation after CO_2 injection, and $b = \ln(C)$. The frequency spectra of these two data sets were calculated using a fast Fourier transform algorithm. The logarithmic spectrum of the direct wave after CO_2 injection is subtracted from the logarithmic spectrum of the direct wave before CO_2 injection. A linear regression line is fit to the data of $Y(f)$ versus frequency. The slope of this line is used to estimate an index of integrated attenuation. The advantages of this method is that we do not require the energy of the source to be the same in two different measurements.

CENTER FREQUENCY SHIFT METHOD

Suppose that the incident spectrum is Gaussian. Then from the centroid frequency shift method (Quan and Harris, 1993), we have

$$\int_{ray} \Delta\alpha_o dl = (f_{1s} - f_{1r}) / \sigma_{1s}^2 - (f_{2s} - f_{2r}) / \sigma_{2s}^2, \tag{8}$$

where f_{is}, f_{ir} and σ_{is}^2 $(i = 1,2)$ are the source and receiver centroid frequencies, and source variance, respectively.

From these two methods, we can estimate the integration attenuation a. Considering that the estimated α_o involves noise, we have the following equation

$$a = (\int_{ray} \Delta\alpha_o dl) + n, \tag{9}$$

where n is the noise term. From (9), we can establish a large linear system of equations and the attenuation distribution can be obtained by solving this linear system. However, as we know, the data in equation (9) usually are highly contaminated with noise. In addition, the measured data have limited aperture. Therefore, the linear system is ill-posed due to the incompleteness of the data and the noise problem. We need robust algorithms to solve this linear system. Considering the fact that conventional regularization methods with smoothing conditions are poor and that it is difficult to choose the regularization factor, we adopt the maximum entropy as the constraining condition in our inversion of equation (9). We use the Maximum Entropy Cambridge Algorithm (Skilling and Bryan, 1984) to find a solution from all solutions which fit the integrated attenuation data.

SYNTHETIC EXAMPLE

We first present a synthetic experiment to test our estimation methods. The synthetic models are shown in Figures 1(a)and 1(b). Figure 1 represents a model before CO_2 injection. We assume that the parameter differences between Figures 1a and 1b are caused by CO_2 injection. The anelastic wave simulation for radially symmetric media (Quan, Chen and Harris, 1996) is used to calculate two complete seismic data sets corresponding to before and after the CO_2 injection.

We then use a short time window to extract the direct P waves (before and after CO_2) and estimate their spectra. Figure 2 shows the spectrum ratio $Y(f)$ of the P waves calculated using equation (7). From the figure, we can see that the relationship between $Y(f)$ and frequency is almost linear. The slope of these lines is the perturbation of the integrated attenuation .

Either equation (7) (slope method) or equation (8) (frequency shift method) can be used to image the perturbation distribution of the attenuation. The imaging of the attenuation perturbation shows the area influenced by the CO_2 injection. Figures 3a and

3b give the attenuation perturbation tomograms obtained by the slope method and the frequency shift method, respectively.

FIELD DATA EXAMPLE – CO_2 INJECTION PILOT

The two field data sets used for this study were collected from the same pair of wells before and after CO2 injection in a west Texas oil field. In order to reduce the interference on the direct arrivals caused by reflections from interfaces, we align and mix adjacent traces in different sorting gathers. Since the reflections exhibit a different moveout than the direct wave, the mixing can significantly reduce the interference and thus the contamination of the direct arrival spectrum. For the field data, we only present

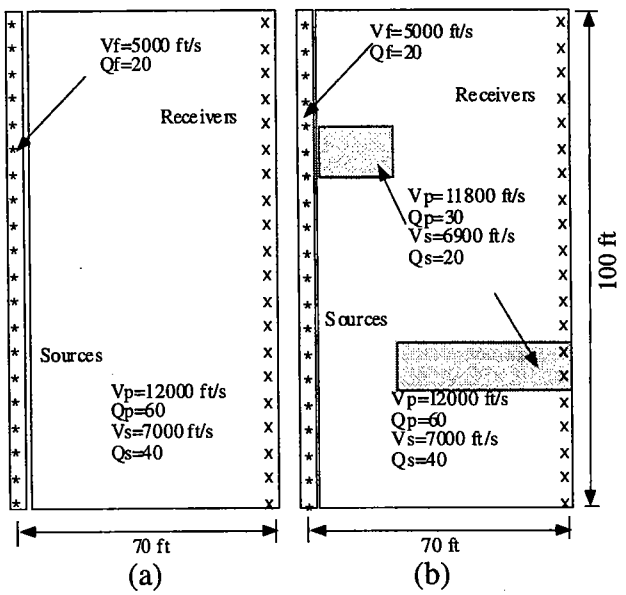

Figure 1. Simulation models before (a) and after (b) injecting CO_2.

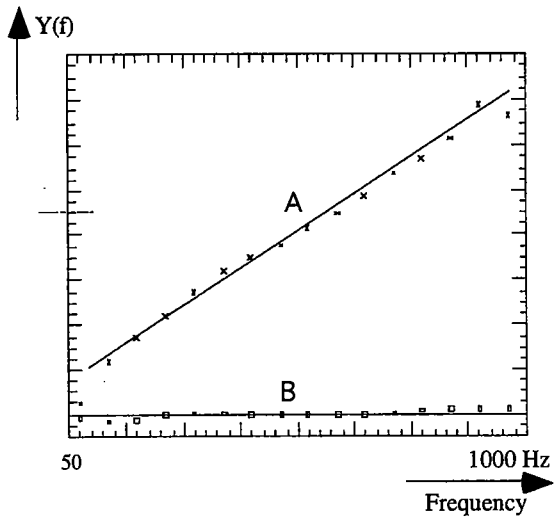

Figure 2. Y(f) in equation (7), as a function of the frequency. Curve A is obtained from the amplitude spectra of a source-receiver pair passing through the injection zone. Curve B is obtained from the amplitude spectra of a source-receiver pair not passing through the changed zone.

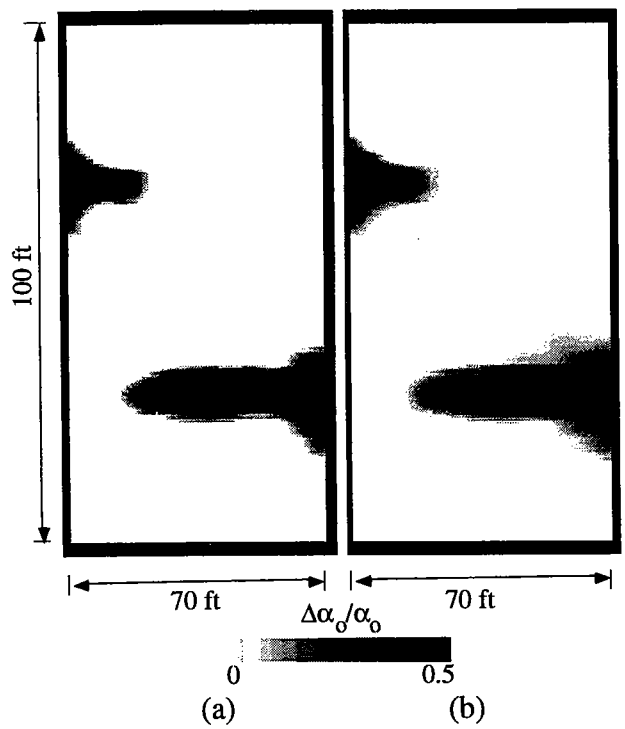

Figure 3. (a) is the *P*-wave relative attenuation derived by the amplitude spectral ratio method; (b) is the *P*-wave relative attenuation derived by the center frequency shift method.

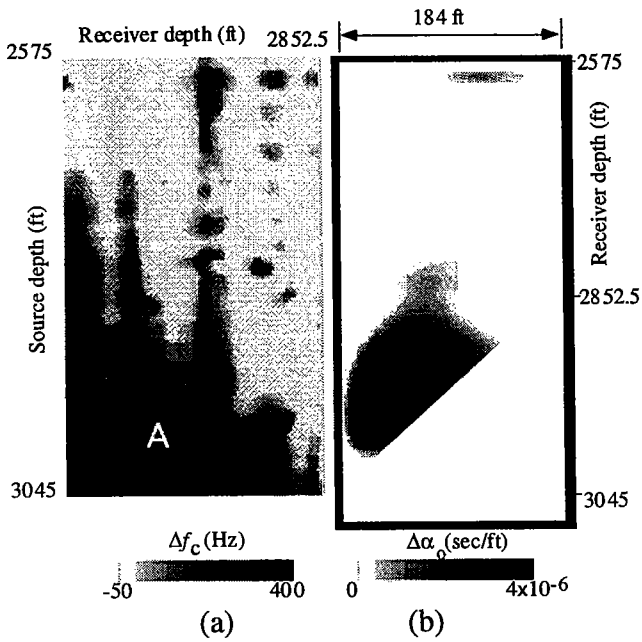

Figure 4. (a) is the center frequency difference map of direct *P*-wave before carbon dioxide injection and after carbon dioxide injection. (b) is the relative *P*-Wave attenuation derived by center frequency method.

the frequency shift method. Figure 4a shows the centroid frequency difference for the data before and after CO_2 injection at the pilot site. The centroid frequency change indicated by letter A is about 300 Hz,. that is, the centroid frequency of the direct *P*-wave passing through the CO_2 injection zone is dramatically decreased by about 25%. Figure 4b is the resulting attenuation perturbation, i.e., change in attenuation caused by the CO_2 injection process. We can see that in the reservoir zone (that is the injection zone) the *P* wave attenuation increase 15-20%. The CO2 effect on attenuation is significant.

CONCLUSIONS

In this paper, we presented two attenuation methods for imaging of a zone where CO_2 was injected for the enhanced oil recovery. We used seismic waves recorded before and after injection in a crosswell geometry to estimate changes in attenuation. The results show that it is possible to detect and image the changes in reservoir attenuation during the course of production for purposes of monitoring the enhanced oil recovery process.

ACKNOWLEDGMENTS

This work was supported by DOE Grant DE-FG03-95ER14535/A000, and sponsors of the McElroy Reservoir Geosciences Project (Amoco, Chevron, Conoco, GRI, Phillips, and Texaco).

REFERENCES

Best, A. I., McCann., and Sothcott, J., The relationships between the velocities, attenuations, and petrophysical properties of reservoir sedimentary rocks: Geophys. Prosp., **42**, 151-178, 1994.

Broome, J. H., Bohannon, J. M., and Stewart, W. C., 1986. The 1984 National petroleum Council Study on EOR: An Overview. JPT, **38**, 869-874.

Cheng, C., Toksoz, N and Willis, M., 1982, Determination of in situ attenuation from full waveform acoustic logs: JGR, **87,** No. B7, 4577-5484.

Engelhard, L., Grass, Th. and Neupert, F., 1984, Comment on " Determination of in situ attenuation from full waveform acoustic logs": JGR, **89**, No. B5, 3400.

Narayana, P.A. and Ophir, J., A closed form for the measurement of attenuation in non linearly dispersive media: Ultrasonic Imaging, **5**, 17-21, 1983.

Pratt R. G. and N. R. Goulty, Combining wave-equation imaging with traveltime tomography to form high-resolution images from crosshole data, Geophysics, **56**, No. 2, 208-224, 1991.

Quan, Y. and Harris, J.M.., 1993, Seismic attenuation tomography based on centroid frequency shift: SEG Extended Abstracts.

Quan, Y., Chen X. and Harris, J. M., 1996, Elastic waves in complex radially symmetric media: SEG Extended Abstracts.

Skilling, J., and Bryan, R.K., 1984, Maximum entropy image reconstruction: general algorithm, Mon. Not. R. Astr. Soc., **211**, 111-124.